Fractal Variability and Heterogeneity of Fracture Surfaces in Steel

B. Strnadel[1] and I. Dlouhý[2]

[1]Technical University of Ostrava, Department of Materials Engineering, 17. listopadu 15, 70833 Ostrava, Czech Republic; e-mail: bohumir.strnadel@vsb.cz
[2]Institute of Physics of Materials, Academy of Sciences, Žižkova 22, 616 62 Brno, Czech Republic; e-mail: idlouhy@ipm.cz

ABSTRACT. *Microstructural effects on the fractality of cracks in steels at low temperatures have been investigated. The fractal analysis of fracture surfaces was conducted employing broken three-point bend test samples of Ni-Cr steel with two states of ferrite microstructure containing fine carbides. Alternation of fractal dimension in the direction of the crack propagation corresponds to characteristic regions ahead of sharp crack tip controlled by different fracture micromechanisms. In the ductile damage region the fractal dimension attains its maximum. In the brittle fracture region the fractal dimension is minimal and it does not change too much with increasing distance from the initial crack tip. Competing effects of the transgranular and intergranular brittle failure can cause growth of surface roughness and its fractal dimension. The fracture toughness of the Ni-Cr steel tested in the transition region is inversely proportional to differences of fractal dimension in stable crack propagation area and in the area of unstable brittle fracture.*

INTRODUCTION

Although a lot of attention has been paid to investigation of damage mechanisms in structural steels [1-3], only a few papers refer to crack kinetics in relation to changes of the mechanism that controls formation of crack surfaces [4-7]. Nevertheless, understanding to conversion patterns of the crack controlling mechanism may be of major importance for utilising of the local dissipation resources of deformation energy for development of new structural steels of enhanced toughness level. Changes of conditions for crack propagation may strongly affect not only stages of failure micromechanism but also combined effects of their interactions. This directly changes character of the local fracture surfaces, and affects their quantitative fractographic parameters.

The condition of conserving dynamic equilibrium between work of external load, elastic deformation energy, energy needed for the crack propagation, and intrinsic kinetic energy of the crack [3], represent starting points for assessing the relation of the crack propagation rate to changes of the mechanism controlling the propagation. Provided the crack driving force remains constant, the increase of the crack propagation rate is connected with dissipation energy decrease and decrease of the crack tip plastic zone. This is one of the

principal causes that convert the mechanism controlling the main cracks initiation and propagation from ductile to brittle failure in low-alloy steels.

Apart from the micromechanism of the main crack propagation, the integral value of dissipation energy also depends on the local stress-strain conditions and microstructural parameters that define these conditions. This is of direct consequence concerning not only local crack propagation rate along a crack front, but also fracture surface roughness, as well as other fractographic parameters including e.g. the Fourier analysis parameters [8] or the fractal dimension of fracture surface [9-14]. It has been shown [10, 12-14] that fractal dimension does not depend only on micromechanisms of failure but also on the stress-strain conditions for development of their individual stages. Nevertheless, referring to micromechanisms controlling failure and its conversion in different stages of the main crack formation, no dependence of fracture surface fractal on the stress-strain state and main crack propagation kinetics has been studied until now.

The objective of this investigation has been to find out in what manner the fractal dimensions of fracture surface vary with increasing distance from a initial crack tip, and, in addition, which microstructural parameters and local stress-strain characteristics are of major influence on the fractal dimension of the fracture surface in relation to dynamics of the crack propagation.

EXPERIMENTAL METHODS AND RESULTS

Commercially produced low-alloy Ni-Cr steel [15] has been employed for investigation. Following a standard heat treatment (940°C/1hr/air; 650°C/10hr/air), additional precipitation annealing was applied for 100 hrs at 650°C so that transcrystalline cleavage fracture would be achieved at low temperatures. After this treatment, the microstructure consisted of fine ferrite grains with carbide precipitate whose particle sizes were in the range from 0.1 to 0.2 μm. This microstructure was designated as ***T.*** The other microstructure was designated as ***I***, it was obtained by annealing at 550°C for 500 hrs and purpose of this treatment was to initiate intercrystalline embrittlement. The processing produced microstructures comparable to the previous case.

Standard three-point bend test specimens with dimensions of 50×25×220 mm were employed for fracture behaviour assessments and fractal analysis of fracture surfaces. For both ***T*** and ***I*** microstructures fracture toughness temperature dependencies [15-17] have been determined. Although thermal treatment used was different for the same steel, the transition temperatures characterising the lowest temperature of ductile initiation occurrence preceding the brittle propagation, t_{DBL}, are almost the same: t_{DBL}~ -100°C. Nevertheless the upper threshold value of the fracture toughness of the state ***T*** is higher by about 20% comparing to state ***I*** [16-17].

The fracture surfaces of selected specimens were subjected to fractographic analyses employing a scanning electron microscope. As anticipated, fracture surfaces of the variant ***T*** tested at -100°C and -90°C close to t_{DBL} showed characteristic fractographic features. The stretch zone and zone of localised plastic strain close to the initial crack tip is followed by an area of stable crack propagation characterised by a fibrous dimple morphology (Fig. 1a)

that reached the depth of about 1 mm in specimen middle-line area. Behind this area, the failure control mechanism converts from ductile to cleavage one characterised by a distinctly rugged transition area (Fig. 1b). The brittle fracture area is characterised by cleavage facets (Fig. 1c). Concerning the state ***I*** the fracture surfaces of specimens tested at -100°C and -80°C have shown morphological features similar to state ***T***. Some features of intercrystalline damage apart from the dominant cleavage fracture morphology (Fig. 1d) have been found as the only difference.

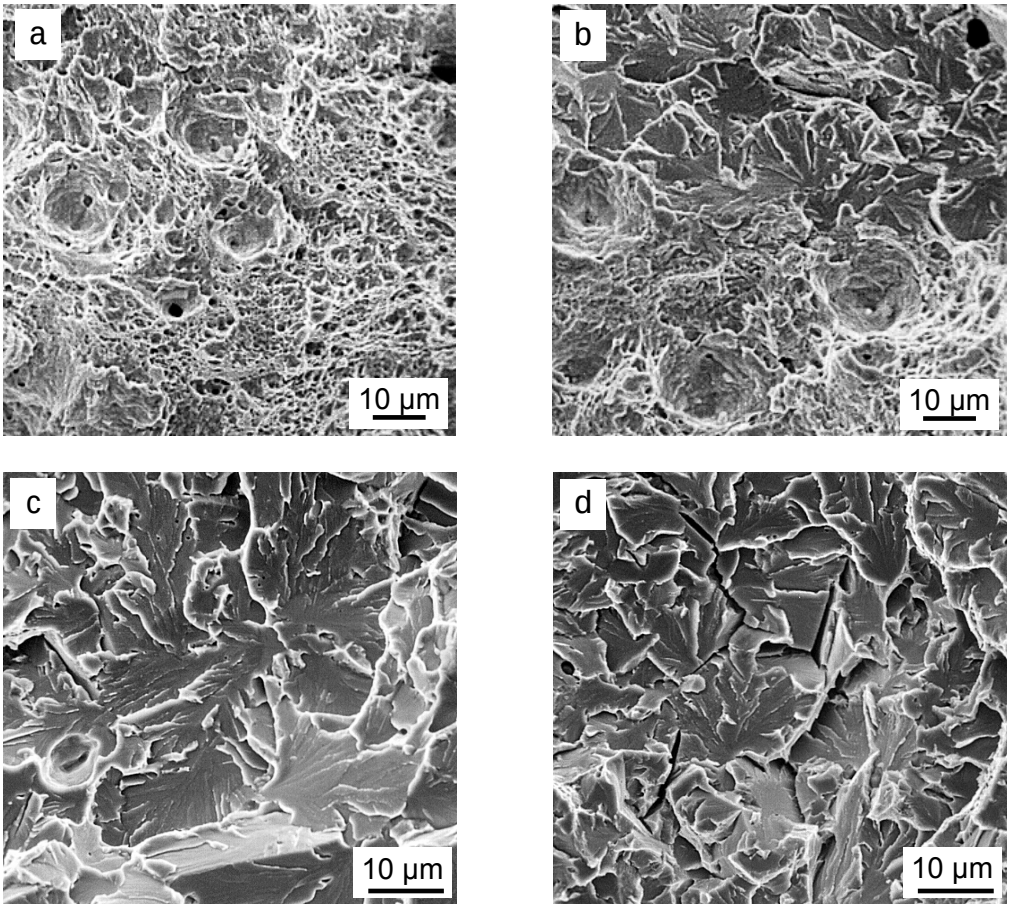

Figure 1. Fractography of the steel: a) ductile fracture close to the blunted crack tip, sample T/-100°C; b) conversion of ductile into cleavage failure, T/-100°C; c) brittle fracture at 0.6 mm from crack tip, I/-100°C; d) brittle fracture at 0.6 mm, I/-100°C.

To establish change of fractal dimension for fracture surfaces below the initial crack tip a method of vertical cuts was employed. The samples were moulded and the metallographic cuts, which included the investigated profile, were made as perpendicular to fracture surfaces. After the preparation, fracture profiles were observed by a light microscope with digital camera. Reductions of about 200 to 300 µm in the direction of the crack propagation then followed in steps and fractal profiles were established for each reduction step. Examples of two fracture profiles for ***T*** and ***I*** states are provided by Figure 2.

Fractal dimensions of fracture profiles, D_F, were obtained by means of a modified Richardson equation [9]:

$$D_F = 1 - \frac{\mathrm{d}\log R_L}{\mathrm{d}\log \eta}, \qquad (1)$$

where R_L is the profile roughness defined as ratio of approximate profile line length, L, to its projection, L_0; $R_L = L/L_0$; and η is the length of yardstick. The dimension D_F was deduced simply from straight line slopes of the logR_L on logη dependences given by pre-defined yardstick lengths, η, and to them related values of roughness, R_L. The definition of the length of yardstick depends on fracture surface ruggedness and sizes of characteristic morphological features [16]. In our case the length of yardstick, η, varied in the range of 8.6 to 34.3 μm. Nevertheless, due to different morphology in area of ductile damage the yardstick range had to be narrower, the values η being only between 3.4 and 13.6 μm. A special numerical software has been developed that enables a direct quantification of the fracture profile roughness, R_L, as a function of the pre-defined length of yardstick, η. An example of this dependence is provided by Figure 3. Even subtle differences in fracture surface morphologies of both variants, ***T*** and ***I***, are reflected by variations of the value D_F.

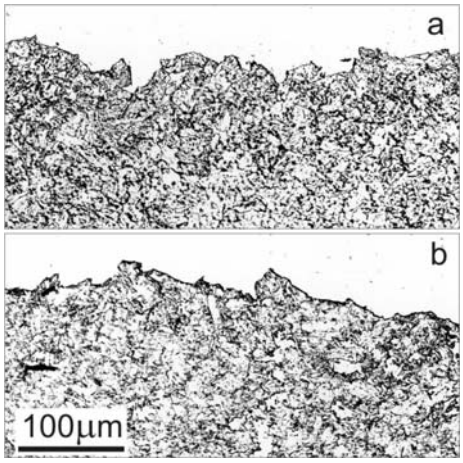

Figure 2. Fracture profile of a) sample T/-100°C at the distance of 1.1 mm and b) sample I/-100°C at 0.9 mm from crack tip

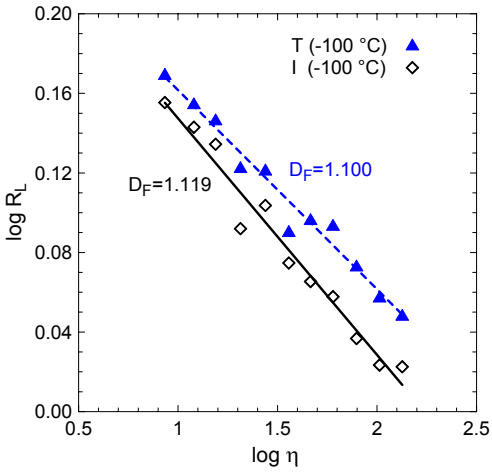

Figure 3. Dependence of fracture profile roughness on the length of yardstick, brittle fracture of samples in Fig. 2

For two specimens of the state ***T*** tested at temperatures of -100°C and -90°C Figure 4 provides the dependencies of the parameter D_F on distances x from the initial crack tip determined in mid-line area of the specimen fracture surface. In the region of unstable transcrystalline brittle fracture there is almost the same value for the dimension D_F, which confirms the effects of analogical damage mechanisms. In this case also the fracture toughness values are more or less the same (K_{Ju} = 488 MPam$^{1/2}$ and 464 MPam$^{1/2}$), although the region of the ductile fracture may perhaps be more extensive for the specimen ***T***/-90°C. The Figure 5 shows similar dependencies for the parameter D_F but the data for state ***I*** are applied. The latter evidences marked differences of the D_F parameter in areas of

brittle damage, and a distinctly wider peak area of the ductile fracture for the specimen, ***I***/-100°C, which also corresponds to a comparably higher value of the fracture toughness (K_{Ju} = 421 MPam$^{1/2}$) comparing to value K_{Ju} = 379 MPam$^{1/2}$ obtained for the specimen, ***I***/-80°C.

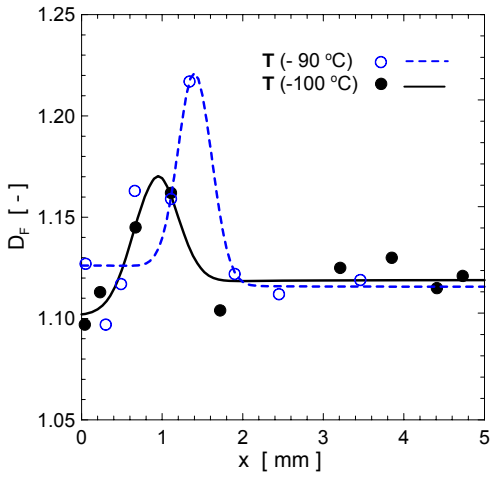

Figure 4. The dependence of fractal dimension, D_F , of fracture surface on distance x from the crack tip for state T.

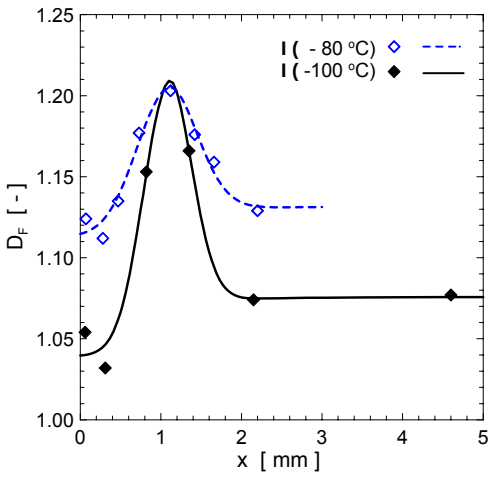

Figure 5. The dependence of the fractal dimension, D_F , on distance x from the crack tip for state I.

Figure 6 illustrates changes of the fractal dimension for profile further away from the initial crack. In distances exceeding five millimetres away from the root, the dimension D_F varies greatly and it is difficult to establish any regularity like that we can identify within the distance of 5 mm from the initial crack tip. The changeful behaviour of D_F in higher distance from the crack tip is most probably caused by different rates of the deformation energy dissipation related to crack propagation, which is very sensitive to local condition of crack initiation and/or propagation.

DISCUSSION

The results have shown that changes in fractal dimension of the fracture profile with distance from the initial crack tip are characterised by three areas corresponding to micromechanisms controlling fracture. The area of stretch zone and shear fracture, as the primary mechanisms of crack initiation, is typical by lower values of the dimension D_F, than in the following area of ductile damage. The values D_F of the fracture profile within the stretch zone generally varied from 1.04 to 1.13, and there was no major difference between both microstructural states of the steel. In the area of the ductile tearing controlled by mechanisms of cavity growth and coalescence nucleated on carbides or other inclusions, the dimension D_F increases, its values are not higher than 1.22 for the state ***T***, and 1.20 for the state ***I***. The results are in good accordance with previous investigations [21]. The final stage of the main crack propagation, which is controlled by brittle fracture mechanisms, is

typical by a sharp drop of the fractal dimension. The lowest value of D_F attained in this area was about 1.07 for the state ***I***, and 1.12 for the state ***T***.

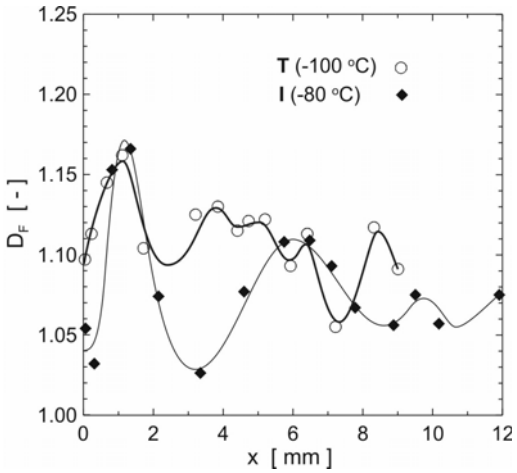

Figure 6. Dependence of the fractal dimension, D_F , on distance x from the crack tip for both states, T and I.

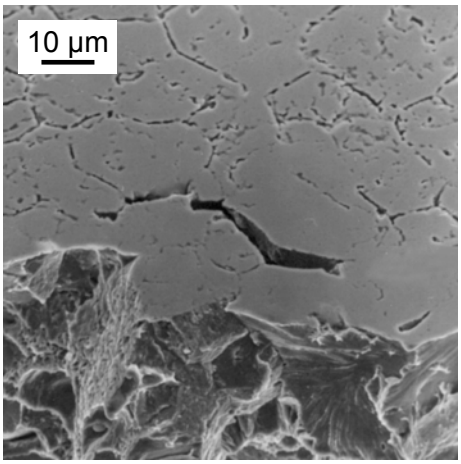

Figure 7. The damage in cross section perpendicular to the fracture surface of the state, I, tested at -100°C.

A graphical summary for selected results provided by Figs. 4-6 correspond to middle part of specimens and plane strain conditions. In spite of these conditions, measurements of the parameter D_F has been affected by local changes of energetic conditions of controlling damage micromechanisms, which are of major influence on the crack orientation (deflection), as well as the character of the crack tip front. Up to a certain point, the dimension D_F is also influenced by the minimal value of the yardstick length. This might be important in ductile crack propagation regime where dimples of dimension comparably less than the length of yardstick are participating on fracture surface formation.

In area of brittle fracture, as documented by Figs. 4–6, relatively small differences of the fractal dimension of the fracture profile with distance from the initial crack tip are observed. In the brittle area and specimen middle part the dimension D_F oscillate within the range of 1.11 to 1.12 for the state ***T***, and 1.07 - 1.13 for the state ***I***. Taking into account relatively small differences in fractal dimension between the two studied states the failure mechanism itself need more attention. The aim of the isothermal annealing (550°C/500 hrs) was to attain a predominantly intercrystalline failure in the transition and lower shelf region of fracture toughness temperature dependence. In fact a special cleavage micromechanism was observed (Fig. 1c); a fracture formed by both cleavage facets and secondary cracks of the sizes not exceeding ferrite grains sizes. A detailed analysis of sub-surface regions showed hidden microcracks at grain boundaries (Figure 7), i.e. in areas in which a cleavage micro-mechanism mainly was in action on the fracture surface. In consequence, the fracture microrelief formation is controlled by competing of two stress-controlled micromechanisms, cleavage transcrystalline and intercrystalline failures. The separate cleavage transcrystalline microcracks are followed by joining affected by intercrystalline

microcracks. The formation of these intercrystalline bridges within cleavage transcrystalline fracture may increase both the fracture surface roughness and thus the value of the dimension D_F. The increased fracture surface roughness would not imply any increases of toughness however. On the contrary, low effective surface energy within intercrystalline area of the state ***I*** can cause fracture toughness decrease comparing to state ***T***.

Relationships of fractal profile dimensions and toughness characteristics are subject of frequent discussions. The outcomes are not always clear-cut. Whereas Mandelbrot et al. [20], as well as many other authors [20-22], have demonstrated an unexpected decrease of the fractal dimension of fracture surface as directly proportional to increasing material fracture toughness; carbon and micro-alloy steels with tempered microstructure [13,23-25], on the contrary, showed increased toughness to be concurrent to increased dimension D_F. Partly the discussed dependence of the dimension D_F on the value of length of yardstick, partly also the fact that current references [13,20-25] do not reflect fractal dimension in relation to changes in crack dynamics and in micromechanism controlling the failures can provide explanation of the differences above mentioned. Apart from this, it is also necessary to take into account that a decisive factor for fracture toughness is the amount of deformation energy stored in the volume under the fracture surface, and varying fracture surface roughness can only affect absolute changes of effective surface energy. The relation between the difference of fractal dimension in area of the stable crack, and that of the unstable brittle fracture and fracture toughness appears to be more appropriate. This idea is also supported by the fact that a decisive factor for converting mechanism of ductile failure into cleavage is given by decreasing strain energy dissipation and contemporary increase of the crack propagation rate. Actually, for state ***T***, a higher value of fracture toughness corresponds to lower peak value in area of the stable crack propagation. In analogy to this, for state ***I***, the value of fracture toughness K_{Ju} = 421 MPam$^{1/2}$ corresponds to lower fractal dimension decrease of only ΔD_F = 0.08; whereas K_{Ju} = 379 MPam$^{1/2}$ corresponds to ΔD_F = 0.15. It is difficult to establish what implications the conversion of the damage mechanism has on changing ratio of the strain energy in the total plastic zone volume to effective surface energy within the total volume of energy dissipation. Nevertheless it is evident that these changes, as it is also documented by a wavy character of the parameter D_F, as illustrated by Fig. 6, will take place.

CONCLUSIONS

The investigation of the fracture surfaces of Ni-Cr steel at temperatures of a lower shelf and transition area provided for the conclusion that the fractal dimension of the fracture profile has, depending on the distance from the initial crack tip, three distinctly characteristic areas that correspond to micromechanisms controlling the failures. In area of the stable crack propagation, the maximum value of the dimension D_F varied from 1.20 to 1.22. Studying relations between fracture toughness and fractal dimension of the Ni-Cr steel with two microstructural states brings out that a major factor influencing these relations is the difference of the dimension D_F in area of stable ductile fracture and area of unstable brittle

fracture. Samples with a higher value of this difference showed lower fracture toughness. Although the fracture toughness is decreasing concurrent action of two competing micromechanisms of transcrystalline and intercrystalline fracture does not necessarily lead to decreased dimension D_F because the secondary intercrystalline cracks increase the fracture profile roughness.

ACKNOWLEDGMENTS

The authors wish to thank the Czech Science Foundation for financial support provided under grant numbers 106/06/0646 and 101/05/0493.

REFERENCES

1. Curry, D. A.: *Metal Sci. 14*, 1980, p. 319.
2. Hahn, G. T.: *Metall. Trans.* A, *15A*, 1984, p. 347.
3. Hahn, G. T., Hoagland, R. G., Kanninen, M. F., Rosenfield, A. R.: *Engng. Fract. Mech.*, *7*, 1975, p. 583.
4. Chen, J. H., Wang, G. Z., Wang, H. J.: *Acta Mater.*, *44*, 1996, p. 3979.
5. Hack, J. E., Chen, S. P., Srolovitz, D. J.: *Acta Metall.*, *37*, 1989, p. 1957.
6. Ishikawa, T., Haze, T.: *Mat. Sci. Engng.*, *A176*, 385.
7. Zhang, X.: *Int. J. Press. Vess. Pip.*, *76*, 1999, p. 583.
8. Coster, M., Chermant, J. L.: *Int. Met. Rev.*, *28*, 1983, p. 228.
9. Banerji, K.: *Metall. Trans. A*, *19A*, 1988, p. 961.
10. Dauskardt, R.H., Haubensak, F., Ritchie, R.O.: *Acta Metall. Mater.*, *38*, 1990, p. 143.
11. Milman, V.Y., Stelmashenko, N. A., Blumenfeld, R.: *Prog. Mat. Sci.*, *38*, 1994, p. 425.
12. Strnadel, B., Byczanski, P.: *Kovove Mater.*, *39*, 2001, p. 93.
13. Jiang, X. G., Chu, W. Y., Hisao, C. M.: *Acta Metall. Mater.*, *42*, 1994, p. 105.
14. Cherepanov, G.P., Balankin, A.S., Ivanova, V.S.: *Engng. Fract. Mech.*,*51*, 1995, p. 997.
15. Dlouhý, I., Němec, O.: In: Proc. of Conf. *Materials Structure and Micromechanics of Fracture* (MSMF-3), Brno, 2001, (Proc. on CD ROM).
16. Němec, O, Dlouhý, I, Strnadel, B: *Kovové Mater.*, 41(3) 2003, p.177.
17. Dlouhý, I., Hadraba, H., Holzmann, M.: In: *Proc. of 16th Europ. Conf. on Fracture*, ECF16, Alexandroupolis, 2006
18. Long, Q. Y., Suqin, L., Lung, C. W.: J. Phys. D: *Appl. Phys.*, *24*, 1991, p. 602.
19. Mandelbrot, B. B., Passoja, D. E., Paullay, A. J.: *Nature*, *308*, 1984, p. 721.
20. Imre, A., Paykossy, T., Nyikos, L.: *Acta Metall. Mater.*, *40*, 1992, p. 1819.
21. Pande, C. S., Richards, L. E., Louat, N., Dempsey, B. D., Schwoeble, A. J.: *Acta Metall.*, *35*, 1987, p. 1633.
22. Przerada, I., Bochenek, A.: *Acta Stereologica*, *11*, 1992, p. 343.
23. Ray, K. K., Mandal, G.: *Acta Metall. Mater.*, *40*, 1992, p. 463.
24. Mu, Z. Q., Lung, C. W.: *Theor. Appl. Fract. Mech.*, *17*, 1992, p. 157.
25. Underwood, E. E., Banerji, K.: *Mater. Sci, Engng.*, *80*, 1986, p. 1.